AJNR

Suprasellar arachnoid cysts: 1. CT recognition.

L R Gentry, W R Smoker, P A Turski, A H Menezes, L Ramirez and S H Cornell

AJNR Am J Neuroradiol 1986, 7 (1) 79-86
http://www.ajnr.org/content/7/1/79

Suprasellar Arachnoid Cysts: 1. CT Recognition

Lindell R. Gentry[1,2]
Wendy R. K. Smoker[1]
Patrick A. Turski[3]
Arnold H. Menezes[4]
Lincoln Ramirez[5]
Steven H. Cornell[1]

Suprasellar arachnoid cysts are basal midline masses that represent a rare but surgically remediable cause of hydrocephalus and neurologic deficits. These cysts represent a diagnostic challenge and often go unrecognized for many years. The authors review the computed tomographic (CT) findings in seven patients with documented suprasellar arachnoid cysts and define previously undescribed diagnostic criteria. These cysts usually can be differentiated from cystic midline neoplasms by their CT density, homogeneity, and location as well as by their lack of fat, lack of calcification, and absence of contrast enhancement. Accurate distinction from marked third-ventricular enlargement secondary to obstructive hydrocephalus and from third-ventricular ependymal cysts can be made on the basis of basal cisternal expansion, distinctive mass effect and displacement, the characteristic shape and contour of the apparent "third ventricle," and the appearance of structures at the foramen of Monro. Although metrizamide CT ventriculography and cisternography allow confirmation of the diagnosis and evaluation of cerebrospinal fluid dynamics, these definitive studies will not be obtained unless the cysts are first suspected by their conventional CT appearance.

Arachnoid cysts account for about 1% of intracranial mass lesions [1], but fewer than 15% are located in the suprasellar region [2–4]. Despite the rarity of these basal midline masses, they represent a surgically treatable cause of neurologic symptoms. Although fewer than 60 cases have been reported [5], we believe suprasellar arachnoid cysts (SSAC) are much more common than these figures would indicate.

Sansregret et al. [6] and Fox and Al-Mefty [7] suggest that the membrane of Liliequist plays a role in the development of most SSAC. This normally perforated, veillike membrane incompletely separates the interpeduncular and chiasmatic parts of the suprasellar cistern, stretching between its attachment points at the dorsum sellae, oculomotor nerves, hypothalamus, and ventral midbrain (fig. 1A). According to their theory, imperforation of this membrane, secondary to congenital maldevelopment or acquired adhesive arachnoiditis, produces obstruction of cerebrospinal fluid (CSF) flow from the infratentorial to supratentorial subarachnoid spaces [7]. The continued egress of CSF from the fourth ventricle causes upward expansion of the membrane in the suprasellar cistern, resulting in formation of a diverticulum that communicates with the pontine cistern (fig. 1B). Further enlargement results in progressive invagination of the diverticulum through the hypothalamus into the third ventricle and even through the foramina of Monro into the lateral ventricles. The diverticulum may retain its communication with the subarachnoid space or the elongated neck may be obliterated or pinched off, resulting in formation of a true cyst (fig. 1C) [5, 7, 8].

Most patients develop symptoms during infancy, secondary to obstructive hydrocephalus [9–12]. Other patients, particularly if hydrocephalus is mild or compensated, may have only minimal or intermittent symptoms, and the diagnosis may go unrecognized until the second or third decade of life [3, 11]. These patients often present with seizures, endocrine dysfunction, or neurologic deficits secondary

Received February 13, 1985; accepted after revision July 7, 1985.

Presented at the annual meeting of the American Society of Neuroradiology, Boston, June 1984.

[1] Department of Radiology, University of Iowa Hospitals and Clinics, Iowa City, IA 52242.
[2] Present address: Department of Radiology, University of Wisconsin Hospitals and Clinics, Madison, WI 53792. Address reprint requests to L. R. Gentry.
[3] Department of Radiology, University of Wisconsin Hospitals and Clinics, Madison, WI 53792.
[4] Department of Neurosurgery, University of Iowa Hospitals and Clinics, Iowa City, IA 52242.
[5] Department of Neurosurgery, University of Wisconsin Hospitals and Clinics, Madison, WI 53792.

AJNR 7:79–86, January/February 1986
0195–6108/86/0701–0079

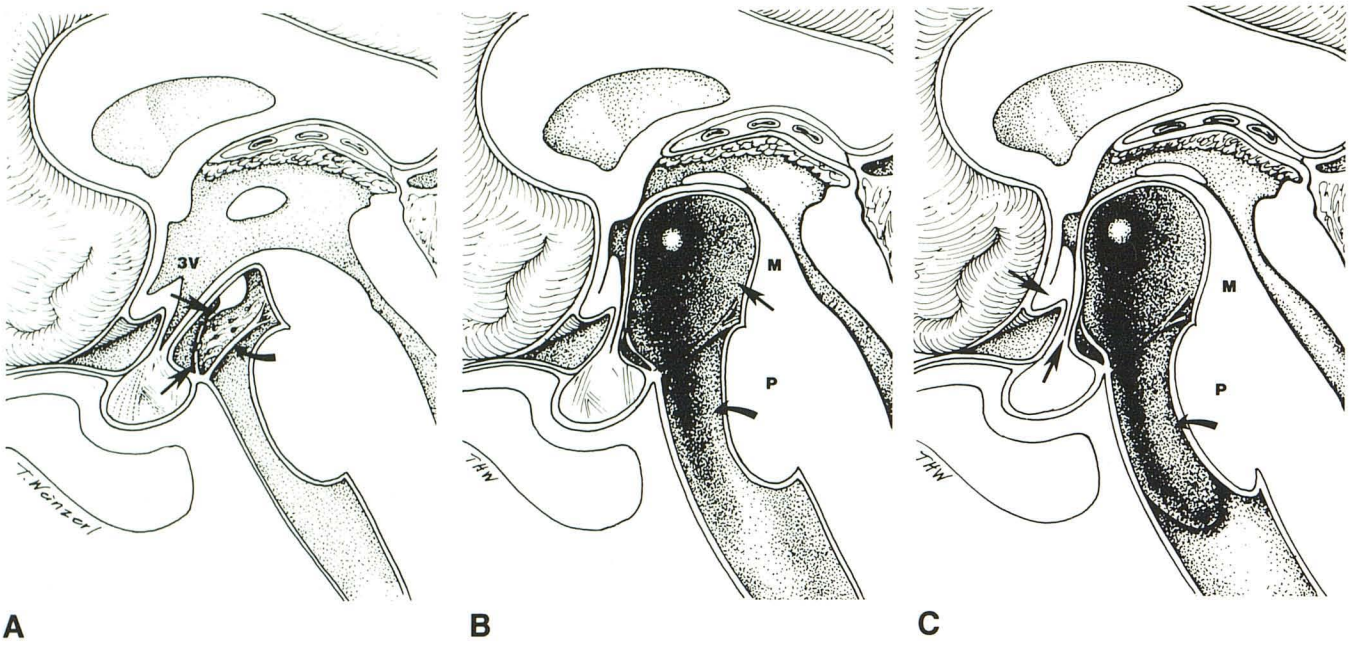

Fig. 1.—Mechanism of development of suprasellar arachnoid cysts (adapted from [7]). **A**, Diagrammatic representation of normally perforated membrane of Liliequist (*straight arrows*) separating chiasmatic and interpeduncular parts of suprasellar cistern. 3V = anterior recesses of third ventricle; *curved arrow* = oculomotor nerve. **B**, Upward expansion of a congenital or acquired imperforate membrane, secondary to continued CSF flow, results in formation of cystic diverticulum (*straight arrow*), which communicates with pontine cistern (*curved arrow*). Diverticulum may invaginate through stretched hypothalamus into anterior aspect of third ventricle, displacing anterior recesses anterosuperiorly. Neck of diverticulum (enlarged pontine cistern) may displace pons (P) and midbrain (M) posteriorly. **C**, Continued expansion results in further compression of pons and midbrain, progressive anterior displacement and compression of optic chiasm and infundibulum (*straight arrows*), and obliteration of anterior aspect of third ventricle. Elongated neck of diverticulum may become obliterated owing to infection, trauma, or hemorrhage, resulting in loss of communication with the subarachnoid space and formation of a true suprasellar and prepontine arachnoid cyst (*curved arrow*).

to compression of adjacent structures by the cyst [3, 11, 12].

The initial diagnosis of SSAC in the modern era is based primarily on recognition at computed tomography (CT). Because of the rarity of SSAC, however, the CT findings of only a few isolated cases have been reported. In 1976, Naidich et al. [13] reported the first case studied with CT as a sharply defined midline mass of CSF density associated with marked obstructive hydrocephalus. Murali and Epstein [14] described three additional cases and stressed the importance of differentiating SSAC from a dilated third ventricle. They emphasized the oval to round appearance of the cyst as a distinguishing feature. Armstrong et al. [12] reported six additional cases and reviewed eight previously reported cases [14–20]. In contrast to previous reports, they found that the rounded shape of the posterior aspect of the cyst was not helpful in differentiating SSAC from third-ventricular enlargement secondary to aqueductal stenosis. They suggested that flattening of the upper brainstem and colliculi may be of value and also emphasized the value of coronal CT and metrizamide ventriculography in the definitive diagnosis. We were able to identify 22 additional cases in the literature, but most of these were isolated case reports [3, 7–10, 21–29].

The initial recognition of SSAC on conventional CT is of critical importance. Although metrizamide-enhanced ventriculography and cisternography are of unquestioned diagnostic value, these studies may not be obtained unless the diagnosis is suspected on the initial CT examination. We present our experience with seven documented cases of SSAC in order to describe several diagnostic CT signs that may aid in initial detection, delineate features that help to differentiate SSAC from other cystic suprasellar masses, and provide guidelines for the selection of patients in whom further investigation with metrizamide-enhanced CT is indicated.

Materials and Methods

Since 1978, eight patients with SSAC have been diagnosed at the hospitals and clinics of the Universities of Iowa and Wisconsin. Seven of these patients had conventional CT examinations as part of their diagnostic evaluation. Excluded from this study were patients with arachnoid cysts confined to the sella turcica or with cysts not located primarily within the suprasellar cistern.

Surgical and pathologic confirmation were available in six cases. Pathologic documentation is not available in the two most recent patients, who have been treated by shunt decompression without operative resection. The diagnoses in these two instances were confirmed by the characteristic appearance of the SSAC at metrizamide-enhanced CT ventriculography and cisternography. In the six patients who had surgical resection, histologic analysis of the cysts revealed walls of variable thickness comprised of fibrocollagenous tissue with an arachnoid lining.

CT evaluations were performed with Picker 600, GE 8800, Siemens Somatom DR3, or EMI 5005 scanners. All seven patients who underwent CT were scanned in the axial plane and two were scanned also in the coronal plane. Five patients were scanned before and all seven were scanned after intravenous administration of contrast medium. Metrizamide CT cisternography and ventriculography were

TABLE 1: **Signs and Symptoms of Suprasellar Arachnoid Cysts in Eight Patients**

Symptom Complex: Location or Type: Symptom	*n*
Compressive:	
Hypothalamo-pituitary:	
Sexual dysfunction/precocious puberty	2
Panhypopituitarism	1
Intermittent diabetes insipidus/obesity	1
Obesity/growth retardation/hyperhidrosis	1
Optochiasmatic:	
Optic atrophy/pallor	6
Visual field deficit	4
Cranial nerve:	
Strabismus	2
Nystagmus	2
Brainstem/cerebral peduncles/thalamus:	
Hyperreflexia/spasticity/Babinski response	5
Extremity weakness	3
Extremity pain/graphesthesia	2
Intermittent hemisensory loss	1
Parinaud syndrome	1
Supranuclear facial palsy	1
Neurobehavioral/psychiatric:	
Personality disorder	4
Hallucinations	2
Seizures	2
Memory loss	1
Cerebellar/basal ganglia:	
Ataxia/clumsiness	4
Tremor	3
Hydrocephalic:	
Headache	6
Lethargy/drowsiness	4
Macrocephaly	3
Nausea/vomiting	2
Papilledema	1
Bobble-head-doll syndrome	1

Note.—Both symptom complexes were present in six patients, only compressive symptoms in one, and only hydrocephalic symptoms in one.

performed in one and two patients, respectively. CT cisternography was performed with 5 ml of metrizamide at a concentration of 170 mg I/ml; for CT ventriculography, 3–4 ml of intraventricular metrizamide (170 mg I/ml) was used.

The five male and two female patients ranged from 8 months to 37 years of age at the time of diagnosis (median, 13 years; mean, 15.6 years).

Results

The signs and symptoms of SSAC among the patients in this series could be divided into two major groups (table 1). *Hydrocephalic* symptoms were predominant in the two youngest patients, but were present to some extent in five of the other six patients. *Compressive* symptoms were predominant in all but one of the six patients who were diagnosed after the age of 5 years. Compression of the hypothalamopituitary axis, optic nerve and chiasm, upper brainstem, cerebral peduncles, basal ganglia, thalamus, cranial nerves, and mesial temporal lobes was responsible for many symptoms in these patients. Both symptom complexes were present in six patients, only compressive symptoms in one, and only hydrocephalic symptoms in one. One patient presented with the bobble-head-doll syndrome, a characteristic rhythmic, 2–3/sec, anterior-to-posterior nodding of the head and trunk, commonly found in patients with SSAC.

The age at onset of neurologic symptoms varied (range, 8 months–35.5 years) but typically began early in life (median, 3 years; mean, 8.75 years). There was usually a long interval between the onset of symptoms and the diagnosis (median, 6 years; mean, 7 years; range, 1 month–21 years). In six of seven instances the SSAC was identified on the initial CT scans, but in one case it was diagnosed only after the cyst had enlarged over a 7-year period. This patient had been evaluated 11 years earlier with pneumoencephalography, at which time extraventricular obstructive hydrocephalus was noted but the suprasellar cyst was not recognized. The age at the time of diagnosis is greater in this series than in many others [3, 9, 11, 12] and underscores the fact that SSAC is not solely a disease of infancy. Patients with nonspecific, minimal, or intermittent symptoms often did not present until the second or third decade of life, particularly if hydrocephalus was not a predominant feature [3].

Unenhanced (five patients) and contrast-enhanced (seven patients) CT scans demonstrated no evidence of fat, calcification, or enhancement of any part of the lesion. The cysts were completely homogeneous and were isodense with CSF in all patients (fig. 2). The walls of the cysts were never visible (even with contrast enhancement) where they were adjacent to neural structures. The walls could be identified, however, where a part of the cyst wall was surrounded by CSF on both sides (when located within the third or lateral ventricles) (fig. 2). Some part of the cyst wall was visible in six of seven patients and was always uniform and very thin. Table 2 summarizes the conventional CT features of SSAC.

Discussion

Diagnostic Pitfalls

Pathologic, surgical, and radiographic pitfalls have resulted in the misdiagnosis of SSAC as ependymal cysts of the third ventricle or as third-ventricular enlargement secondary to either aqueductal stenosis or extraventricular obstructive hydrocephalus [3].

Pathologic misdiagnosis most often occurs when the superior aspect of the cyst is biopsied by way of a transventricular route or when the dome of the cyst is extensively resected [3]. The superior wall of a cyst that has invaginated into the third ventricle consists of an inner layer of arachnoid and an adherent outer layer, comprising the thinned hypothalamus and the ependymal lining of the floor of the third ventricle. Ependyma, therefore, is expected to line the outer wall of an SSAC that has been biopsied by a transventricular approach. The correct diagnosis can be made only if care is taken to identify correctly the inner wall of the cyst at biopsy and histologic examination [8]. Thus, it is not surprising that many SSAC that have invaginated into the third ventricle are misdiagnosed as ependymal cysts [3].

For similar reasons, SSAC often is misdiagnosed at surgery. The third-ventricular part of the SSAC will have an apparent broad-based attachment to the floor of the third ventricle, suggesting an intraventricular origin [7]. If its true origin is not recognized, the dome of the cyst, consisting in

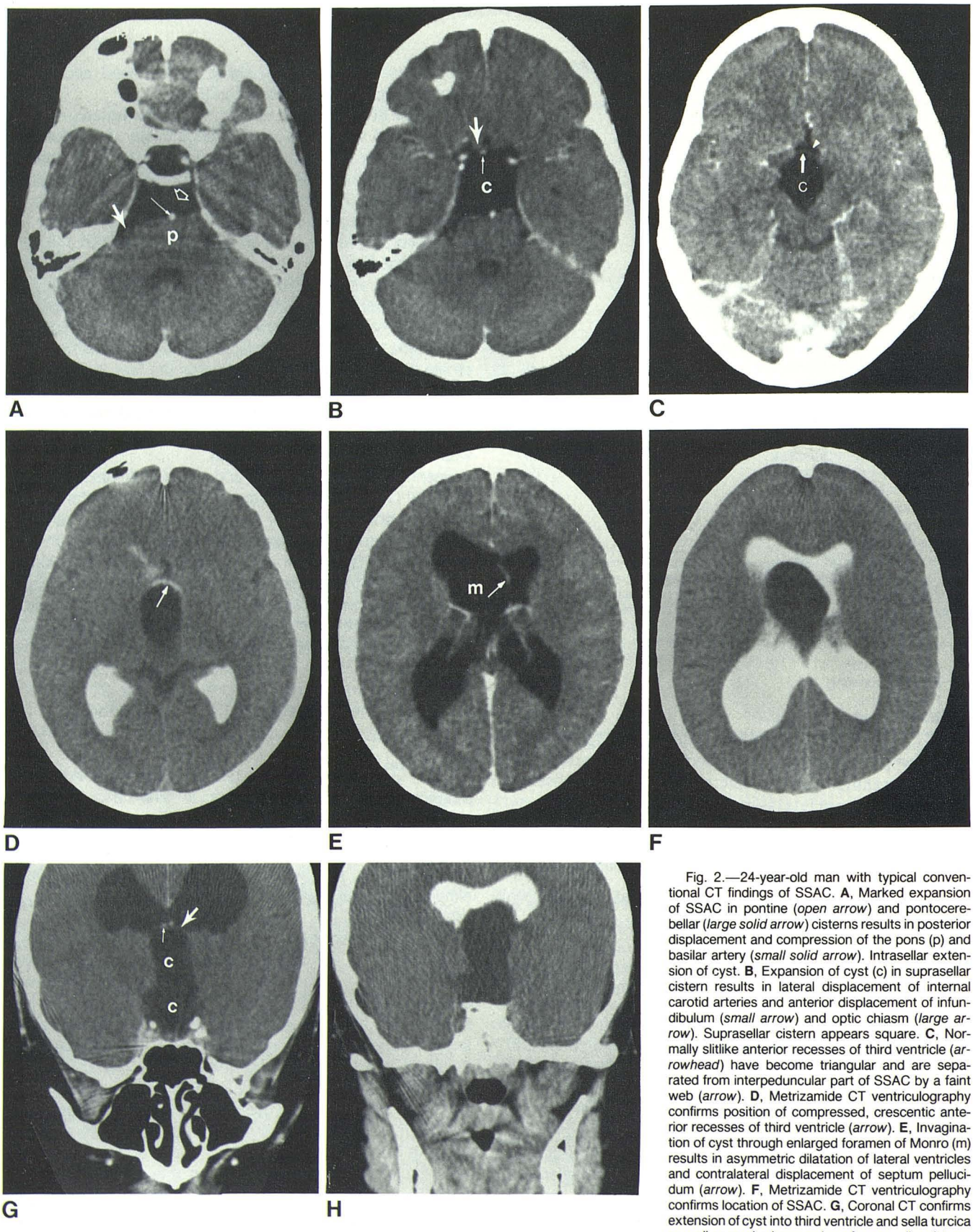

A B C

D E F

G H

Fig. 2.—24-year-old man with typical conventional CT findings of SSAC. **A**, Marked expansion of SSAC in pontine (*open arrow*) and pontocerebellar (*large solid arrow*) cisterns results in posterior displacement and compression of the pons (p) and basilar artery (*small solid arrow*). Intrasellar extension of cyst. **B**, Expansion of cyst (c) in suprasellar cistern results in lateral displacement of internal carotid arteries and anterior displacement of infundibulum (*small arrow*) and optic chiasm (*large arrow*). Suprasellar cistern appears square. **C**, Normally slitlike anterior recesses of third ventricle (*arrowhead*) have become triangular and are separated from interpeduncular part of SSAC by a faint web (*arrow*). **D**, Metrizamide CT ventriculography confirms position of compressed, crescentic anterior recesses of third ventricle (*arrow*). **E**, Invagination of cyst through enlarged foramen of Monro (m) results in asymmetric dilatation of lateral ventricles and contralateral displacement of septum pellucidum (*arrow*). **F**, Metrizamide CT ventriculography confirms location of SSAC. **G**, Coronal CT confirms extension of cyst into third ventricle and sella turcica as well as marked expansion of suprasellar cistern. Thin upper wall of cyst (*large arrow*) causes superior displacement of internal cerebral veins (*small arrow*). **H**, Metrizamide CT ventriculography confirms superior extent of cyst.

TABLE 2: **CT Features of Suprasellar Arachnoid Cysts in Seven Patients**

Type or Location of Finding: CT Feature	*n*
Cyst characteristics:	
Homogeneous	7
Isodense with CSF	7
Wall of cyst visible	6
Thin uniform wall	6
Fat	0
Calcification	0
Enhancement	0
Dilatation of basal cisterns:	
Suprasellar	7
Pontine	6
Pontocerebellar	5
Intrasellar extension	4
Trigeminal	1
Crural	1
Parasellar mass effect/displacement:	
Anterolateral displacement of carotid arteries	7
Posterior displacement of basilar artery	6
Posterior displacement of pons/midbrain	6
Splaying of cerebral peduncles	6
Anterior flattening or concavity of pons	5
Anterior displacement of chiasm/infundibulum	5
Posterior displacement of optic chiasm	1
Characteristics of apparent third ventricle:	
Anterior third-ventricular "web"	6
Triangular-shaped anterior recesses	6
Diamond-shaped mid-third ventricle	6
Disproportionately small suprapineal recess	6
Disproportionate enlargement of third ventricle (as compared to lateral ventricles)	5
Continuous with suprasellar cistern	3
Intraventricular region:	
Foramen of Monro "web"	6
Columns of fornix separated and displaced upward	6
Unilateral foramen of Monro enlargement	5
Lateral displacement/buckling of septum pellucidum	4
Cavum septi pellucidi	2
Ventricular system:	
Asymmetric lateral-ventricular dilatation	3
Fourth-ventricular enlargement	1

part of the thinned hypothalamus, may be resected. It is therefore not surprising that diabetes insipidus and hypothalamic dysfunction often result from extensive surgical resection of the dome of SSAC [9–11].

Radiologic misdiagnosis may occur with CT, air or positive-contrast ventriculography, pneumoencephalography, and metrizamide CT cisternography or ventriculography. Entry of air (at pneumoencephalography) or metrizamide (at CT cisternography) into the midline cyst, which has invaginated into the third ventricle, may result in misidentification of the cyst as the third ventricle. In one of our patients the cyst, aqueduct, third ventricle, and lateral ventricles all filled with air at pneumoencephalography. The paper-thin wall of the cyst was not recognized in this patient, resulting in misdiagnosis of the SSAC as communicating (extraventricular) obstructive hydrocephalus and an 11-year delay in the correct diagnosis. SSAC can be mistaken for third-ventricular ependymal cysts at ventriculography or metrizamide-enhanced CT ventriculography [3].

CT Findings

A knowledge of the manner of formation, mechanism of growth and expansion, and characteristic areas of involvement by SSAC is beneficial in understanding the typical CT appearance of these lesions. Recognition of characteristic findings on standard enhanced and unenhanced CT scans will usually allow one to confidently make the diagnosis of SSAC. CT scans usually provide sufficient information for recognizing the cyst and differentiating it from other cystic, basal, midline masses. Each individual finding may not be diagnostic in itself, but most cases of SSAC present with many CT findings, which together provide compelling diagnostic evidence. Although metrizamide CT cisternography and ventriculography are of great value for diagnostic confirmation and preoperative investigation of CSF dynamics [5, 12, 14, 16, 24], these more sophisticated studies may never be obtained if the SSAC is not recognized on the initial conventional CT examination.

General characteristics and differential diagnosis.—Unenhanced and contrast-enhanced CT usually serves to differentiate SSAC from other cystic, suprasellar, midline masses [13, 23, 30–33]. The major entities that must be excluded are craniopharyngioma or Rathke's cleft cysts; neuroepithelial (colloid) cysts; midline neoplasms of maldevelopmental origin (epidermoid, dermoid, lipoma, teratoma); cystic pituitary adenomas; low-grade gliomas of the third ventricle; ependymal cysts of the third ventricle; parasitic cysts (cysticercosis, echinococcal); and massive third-ventricular enlargement from aqueductal stenosis or extraventricular obstructive hydrocephalus.

In our series, SSAC always appeared as rounded, well demarcated, thin-walled, homogeneous, cystic masses that were isodense with CSF (fig. 3). They did not contain areas of calcification or fat and did not enhance with intravenous administration of contrast medium. The lack of calcification, fat, and enhancement allows differentiation from cystic neoplasms such as craniopharyngioma, dermoid, lipoma, teratoma, pituitary adenoma, and low-grade gliomas [13, 23, 30–33]. Although we have not encountered any suprasellar epidermoid tumors that could not be differentiated from SSAC, the literature suggests that the CT features of these lesions, in many instances, may be similar [30]. Like SSAC, epidermoids usually lack calcification and fat, may be homogeneous, often are isodense with CSF, and may not show significant enhancement. However, accurate distinction in difficult cases may be possible if other distinguishing features of SSAC (table 2) are present. Metrizamide CT cisternography also may be useful for differentiation. The inner walls of arachnoid cysts have a smooth, regular margin whereas the interstices of epidermoid tumors have an irregular, lobulated, cauliflower-like appearance. This appearance is due to penetration of metrizamide through the capsule and into the deep, lobulated clefts of these tumors [34, 35].

Differentiation of SSAC from ependymal cysts of the third ventricle, parasitic cysts, or marked third-ventricular enlargement may be difficult on the basis of their general CT features. Echinococcal or cysticercosis cysts [31, 32] may be inhomogeneous, partly calcified, or may enhance slightly. However,

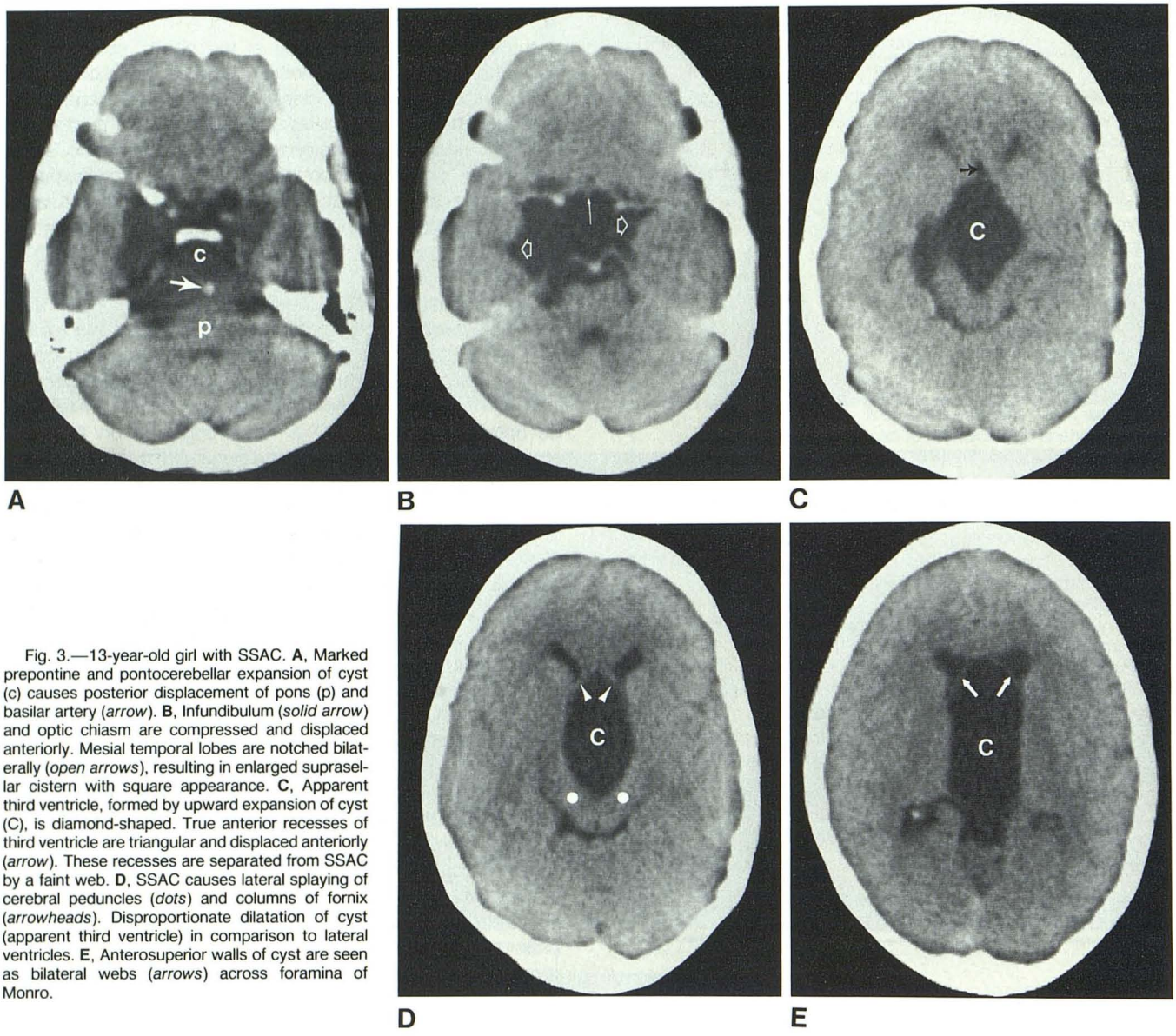

Fig. 3.—13-year-old girl with SSAC. **A**, Marked prepontine and pontocerebellar expansion of cyst (c) causes posterior displacement of pons (p) and basilar artery (*arrow*). **B**, Infundibulum (*solid arrow*) and optic chiasm are compressed and displaced anteriorly. Mesial temporal lobes are notched bilaterally (*open arrows*), resulting in enlarged suprasellar cistern with square appearance. **C**, Apparent third ventricle, formed by upward expansion of cyst (C), is diamond-shaped. True anterior recesses of third ventricle are triangular and displaced anteriorly (*arrow*). These recesses are separated from SSAC by a faint web. **D**, SSAC causes lateral splaying of cerebral peduncles (*dots*) and columns of fornix (*arrowheads*). Disproportionate dilatation of cyst (apparent third ventricle) in comparison to lateral ventricles. **E**, Anterosuperior walls of cyst are seen as bilateral webs (*arrows*) across foramina of Monro.

they rarely share all the features of SSAC (table 2). Distinction of SSAC from marked third-ventricular enlargement and ependymal cysts of the third ventricle is difficult, particularly when there is significant invagination of the cyst into the third ventricle. Accurate differentiation of these two entities from SSAC requires recognition of other characteristic features.

Dilatation of basal cisterns.—The progressive dilatation of the cisterns below an obstructing, imperforate membrane of Liliequist (or other arachnoidal web) was a consistent feature on CT in all seven of our patients. The suprasellar cistern was enlarged and abnormally shaped in every case. The normal five- or six-pointed, star-shaped, suprasellar cistern [13] typically became more oval or square (figs. 2B and 3B). The change in shape was primarily the result of notching and lateral displacement of the mesial temporal lobe and flattening and posterior displacement of the brainstem. Occasionally the cysts extended asymmetrically into the sylvian and crural cisterns, resulting in prominence of one point of the suprasellar "star."

The interpeduncular and pontine cisterns also were consistently enlarged. Enlargement of these cisterns resulted in a superficial resemblance to brainstem atrophy (figs. 2A and 3A). The normal size and shape of the brainstem and the evidence of mass effect (posterior displacement of the brainstem and "splaying" of the cerebral peduncles) serve to differentiate SSAC from cisternal expansion due to atrophy. The cerebellopontine angle cisterns often were asymmetrically enlarged (fig. 2A). Less commonly, the crural and trigeminal cisterns were expanded. In four patients, invagination of the SSAC through the diaphragma sellae resulted in an appearance indistinguishable from that of a partly "empty" sella (fig. 2A). Intrasellar invagination of SSAC has been noted [17, 25].

Expansion of the basal cisterns is very helpful in differen-

tiating SSAC from third-ventricular ependymal cysts or from massive third-ventricular enlargement associated with obstructive hydrocephalus. Cisternal expansion rarely occurs with ependymal cysts or aqueductal stenosis because of the severe intraventricular CSF obstruction. It can occur with extraventricular obstructive hydrocephalus but not, in our experience, to the degree that it is seen with SSAC. In questionable cases, other distinguishing features (table 2) may assist in differentiation of these two entities.

Parasellar mass effect and displacement.—Enlargement of the cysts in the pontine and interpeduncular cisterns resulted in posterior displacement of the basilar artery and brainstem on CT in six of our seven cases. The brainstem displacement was always maximal at the midbrain level. The pons was abnormally flat or even concave in six patients, reflecting the mass effect (fig. 2B). Six patients demonstrated medial concavity or flattening and lateral displacement (splaying) of the cerebral peduncles secondary to marked expansion of the cysts in the interpeduncular cisterns (figs. 2C and 3D). We have encountered similar mass effect with posterior extension of suprasellar neoplasms into the pontine and interpeduncular cisterns, but never with isolated, marked third-ventricular enlargement accompanying intra- or extraventricular obstructive hydrocephalus.

Expansion of the cysts in the suprasellar cisterns also resulted in characteristic mass effect. A part of the cyst typically extended between the optic chiasm and supraclinoid internal carotid arteries, resulting in anterior and lateral displacement of the carotid termination to the lateral margins of the suprasellar cistern (fig. 2B). The infundibulum and optic chiasm could be identified at CT in six of seven cases; in five of these, they were markedly displaced and flattened anteriorly (figs. 2B and 3B). Those cysts thought to be of congenital origin always resulted in anterior displacement of the optic chiasm.

Posterior displacement of the optic chiasm was noted at CT and confirmed at surgery in one patient, a 37-year-old man with bilateral optic atrophy and visual loss. This cyst was different from those in the other six cases in that it appeared to arise anterior to the optic chiasm, was smaller than any of the others, occurred later in life, was not symptomatic from infancy, and did not invaginate into the third ventricle. For these reasons and because of the somewhat thickened arachnoid membranes found at surgery, this case (case 1 [5]) is most likely an acquired cyst, secondary to previous unrecognized trauma or infection.

Characteristics of the apparent "third ventricle."—Analysis of the shape, contour, and size of the apparent "third ventricle" also provides valuable clues to the correct diagnosis. The CT changes reflect the invagination of the cyst through the thinned and attenuated hypothalamus into the anterior aspect of the true third ventricle.

As opposed to true third-ventricular enlargement accompanying aqueductal stenosis, the apparent third ventricle of SSAC was usually dilated out of proportion to the rest of the ventricular system (fig. 3D). This finding was present in the five oldest patients of our series but was not evident in the two youngest patients, who presented with acute hydrocephalus and proportional enlargement of the third and lateral ventricles.

Another common feature of SSAC was disproportionately less dilatation of the suprapineal recess of the apparent third ventricle. The severe compression of the anterior third ventricle and obstruction of the foramina of Monro by the SSAC appears to "protect" the posterior recesses of the third ventricle from marked expansion [5]. This is in sharp contrast to aqueductal stenosis, which usually is associated with marked dilatation of the normally very compliant suprapineal recess [4].

Posterior mass effect by the SSAC also results in a change in the shape of the anterior recesses of the third ventricle from a slitlike structure, oriented in the sagittal plane, to a triangular cavity with the base directed posteriorly (figs. 2C and 3C). As opposed to the compressed, triangular to crescent-shaped appearance with SSAC, they are ovoid and greatly dilated with aqueductal stenosis. In addition, the dilatation of the chiasmatic recess, which lies anterior and superior to the optic chiasm, will displace the chiasm inferiorly and posteriorly in aqueductal stenosis, in contradistinction to SSAC. The anterior wall of the cyst was visible as a "web" between the compressed anterior recesses of the third ventricle and the cyst in six of seven patients (figs. 2C and 3C). The presence of a web in the anterior third-ventricular region does not occur with third-ventricular enlargement secondary to aqueductal stenosis.

The midportion of the "third ventricle" had a characteristic diamond shape in six patients (figs. 2C and 3C). The posterior apex was formed by the splayed cerebral peduncles; the anterior apex by the triangular, compressed anterior recesses of the true third ventricle; and the lateral margins by the junction of the base of the cerebral peduncles and the thalamus. A diamond-shaped mid-third ventricle, in our experience, is rare in aqueductal stenosis.

Coronal CT scans, obtained in three patients, demonstrated continuity of the suprasellar cistern with the apparent third ventricle. The superior wall of the cyst and true floor of the third ventricle were usually markedly displaced upward to the level of the roof of the third ventricle and internal cerebral vein (figs. 2G and 2H).

Intraventricular region and lateral ventricles.—Upward invagination of the SSAC into the anterior aspect of the third ventricle resulted in obstruction of the foramina of Monro in six of seven patients. This was evident as bilateral enlargement of the lateral ventricles. The obstruction was often more severe on one side, resulting in asymmetric dilatation of the lateral ventricles (fig. 2E). Asymmetric expansion of the cyst through one foramen of Monro also could be recognized by ipsilateral enlargement of that foramen and contralateral displacement or buckling of the septum pellucidum (fig. 2E). The anterosuperior walls of the SSAC usually were seen as obstructing membranes or webs across the foramina of Monro (fig. 3E). Untreated aqueductal stenosis is rarely associated with any of these changes.

The superior extension of the cyst from the suprasellar cistern into the anterior aspect of the third ventricle commonly resulted in superior displacement and lateral separation of the

anterior columns of the fornix (fig. 3D). The separation was always maximal inferiorly. We have noted these findings in other large suprasellar neoplasms, but they usually can be differentiated from SSAC by other features such as density, calcification, fat, and enhancement. Third-ventricular enlargement secondary to aqueductal stenosis, in our experience, does not cause this degree of upward displacement or separation of the anterior columns of the fornix.

In summary, the CT differentiation of SSAC from suprasellar cystic neoplasms is usually possible by the homogeneous appearance of SSAC, their similarity in density to CSF, visualization of the paper-thin walls of the cysts where they are adjacent to the lateral or third ventricles, and the lack of calcification, lack of fat, and absence of enhancement. Although SSAC may bear a superficial resemblance to a dilated third ventricle associated with aqueductal stenosis, they can be differentiated on the basis of the shape and contour of the apparent third ventricle, characteristic parasellar mass effect and displacement of adjacent structures, and distinctive basal cisternal expansion. Detection of this unusual but treatable cause of hydrocephalus and neurologic deficit depends on the recognition of these characteristic findings on conventional CT. Definitive diagnosis and pretherapeutic characterization of the CSF dynamics [5, 12] by metrizamide CT cisternography or ventriculography can then be obtained.

REFERENCES

1. Robinson RG. Congenital cysts of the brain: arachnoid malformations. *Prog Neurol Surg* **1971**;4:133–174
2. Menezes AH, Bell WE, Perret GE. Arachnoid cysts in children. *Arch Neurol* **1980**;37:168–172
3. Gonzalez CA, Villarejo FJ, Blazquez MG, Castroviejo IP, Higueras AP. Suprasellar arachnoid cysts in children—report of 3 cases. *Acta Neurochir* (Wien) **1982**;60:281–296
4. Harwood-Nash DC, Fitz CR. Intracranial cysts. In: *Neuroradiology in infants and children.* St. Louis: Mosby, **1976**:965–997
5. Gentry LR, Menezes AH, Smoker WRK, Turski PA, Cornell SH, Ramirez L. Suprasellar arachnoid cysts: 2. Evaluation of CSF dynamics. *AJNR* **1986**;7:87–96
6. Sansregret A, Ledoux R, Duplantis F, Lamoureux C, Chapdelaine A, Leblanc P. Suprasellar subarachnoid cysts: radioclinical features. *AJR* **1969**;105:291–297
7. Fox JL, Al-Mefty O. Suprasellar arachnoid cysts: an extension of the membrane of Liliequist. *Neurosurgery* **1980**;7:615–618
8. Binitie D, Williams B, Case CP. A suprasellar subarachnoid pouch: aetiological considerations. *J Neurol Neurosurg Psychiatry* **1984**;47:1066–1074
9. Raimondi AJ, Shimoji T, Gutierrez FA. Suprasellar cysts: surgical treatment and results. *Childs Brain* **1980**;7:57–72
10. Cilluffo JM, Onofrio BM, Miller RH. The diagnosis and surgical treatment of intracranial arachnoid cysts. *Acta Neurochir* (Wien) **1983**;67:215–229
11. Hoffman HJ, Hendrick EB, Humphreys RP, Armstrong EA. Investigation and management of suprasellar arachnoid cysts. *J Neurosurg* **1982**;57:597–602
12. Armstrong EA, Harwood-Nash DCF, Hoffman H, Fitz CR, Chuang S, Pettersson H. Benign suprasellar cysts: the CT approach. *AJNR* **1983**;4:163–166
13. Naidich TP, Pinto RS, Kushner MJ, et al. Evaluation of sellar and parasellar masses by computed tomography. *Radiology* **1976**;120:91–99
14. Murali R, Epstein F. Diagnosis and treatment of suprasellar arachnoid cyst: report of 3 cases. *J Neurosurg* **1979**;50:515–518
15. Lee BCP. Intracranial cysts. *Radiology* **1979**;130:667–674
16. Leo JS, Pinto RS, Hulvat GF, Epstein F, Kricheff II. Computed tomography of arachnoid cysts. *Radiology* **1979**;130:675–680
17. Kasdon DL, Douglas EA, Brougham MF. Suprasellar arachnoid cyst diagnosed pre-operatively by computerized tomographic scanning. *Surg Neurol* **1977**;7:299–303
18. Wirt TC, Hester RW. Suprasellar arachnoid cysts. *Surg Neurol* **1978**;9:322
19. Handa J, Nakano Y, Heiha A. CT cisternography with intracranial arachnoid cysts. *Surg Neurol* **1977**;8:451–454
20. Anderson FM, Segall HD, Caton WL. Use of computerized tomography scanning in supratentorial arachnoid cysts: a report on 20 children and 4 adults. *J Neurosurg* **1979**;50:323–338
21. Gyldensted C, Karle A. Computed tomography of intra- and juxtasellar lesions: a radiological study of 108 cases. *Neuroradiology* **1977**;14:5–13
22. Lesser RL, Geehr RB, Higgins DD, Greenberg AD, Ocular motor paralysis and arachnoid cyst. *Arch Ophthalmol* **1980**;98:1993–1995
23. Miller JH, Pena AM, Segall HD. Radiological investigation of sellar region masses in children. *Radiology* **1980**;134:81–87
24. Ruscalleda J, Guardia E, dos Santos FM, Carvajal A. Dynamic study of arachnoid cyst with metrizamide. *Neuroradiology* **1980**;20:185–189
25. Harter LP, Silverberg GD, Brant-Zawadzki M. Intrasellar arachnoid cyst: case report. *Neurosurgery* **1980**;7:387–390
26. Kishore PRS, Krishna Rao CVG, Williams JP, Vines FS. The limitation of computerized tomographic diagnosis of intracranial midline cysts. *Surg Neurol* **1980**;14:417–431
27. McCullough DC, Harbert JC, Manz HJ. Large arachnoid cysts at the cranial base. *Neurosurgery* **1980**;6:76–81
28. Giudicelli G, Hassoun J, Choux M, Tonon C. Supratentorial "arachnia" cysts. *J Neuroradiol* **1982**;9:179–201
29. Kline LB, Vitek JJ, Acker JD. Computed tomography in the evaluation of the optic chiasm. *Surv Ophthalmol* **1983**;27:387–396
30. Zimmerman RA, Bilaniuk LT. Cranial computed tomography of epidermoid and congenital fatty tumors of maldevelopment origin. *J Comput Tomogr* **1979**;3:40–50
31. Zee C, Segall HD, Miller C, et al. Unusual neuroradiological features of intracranial cysticercosis. *Radiology* **1980**;137:397–407
32. Byrd SE, Locke GE, Biggers S, Percy AK. The computed tomographic appearance of cerebral cysticercosis in adults and children. *Radiology* **1982**;144:819–823
33. Dietemann JL, Bonneville JF, Buchheit F, Cattin F, Heldt N, Wackenheim A. CT findings in symptomatic Rathke's cleft cysts of the pituitary gland. *Neuroradiology* **1983**;24:263–267
34. Hiratsuka H, Okada K, Matsunaga M, Tanaka K, Fukai N, Inaba Y. Diagnosis of epidermoid cysts by metrizamide CT cisternography. *Neuroradiology* **1984**;26:153–155
35. Inoue H, Toya SH, Ohtani M, et al. Characteristic findings of metrizamide CT cisternography in epidermoids. *Acta Neurochir* **1984**;73:207–211